analytical chemistry

Article

Cite This: *Anal. Chem.* 2018, 90, 8028−8034

pubs.acs.org/ac

Ferritin-Triggered Redox Cycling for Highly Sensitive Electrochemical Immunosensing of Protein

Md. Rajibul Akanda[†] and Huangxian Ju*

State Key Laboratory of Analytical Chemistry for Life Science, School of Chemistry and Chemical Engineering, Nanjing University, Nanjing 210023, P. R. China

Supporting Information

ABSTRACT: Electrochemical immunoassay amplified with redox cycling has become a challenging topic in highly sensitive analysis of biomarkers. Here a ferritin-triggered redox cycling is reported by using a highly outersphere reaction-philic (OSR-philic) redox mediator ruthenium hexamine ($Ru(NH_3)_6^{3+}$) to perform the OSR-philic/innersphere reaction-philic (ISR-philic) controlled signal amplification. The screened mediator can meet the needs of lower $E^{0\prime}$ than ferritin, low reactivity with ISR-philic species, and quick electron exchange with ferritin redox couple. The ferritin-labeled antibody is first bonded to immunosensor surface by recognizing the target antigen capured by the immobilized primary antibody. The ferritin then mediates OSR-philic/ISR-philic transfer from $Ru(NH_3)_6^{3+/2+}$/immunosensor to ferritin-H_2O_2 redox system. The fast mediation and excellent resistant of highly OSR-philic $Ru(NH_3)_6^{3+}$ against radical oxygen species lead to highly sensitive electrochemical readout and high signal-to-background ratio. The proposed redox cycling greatly enhances the readout signal and the sensitivity of traditional ferritin-labeled sandwich immunoassay. Using Enteropathogenic coli (*E. coli*) antigen as a model analyte, the developed method shows excellent linearity over the concentration range from 10.0 pg/mL to 0.1 μg/mL and a detection limit of 10.0 fg/mL. The acceptable accuracy, good reproducibility, and selectivity of the proposed immunoassay method in real samples indicate the superior practicability of the ferritin-triggered redox cycling.

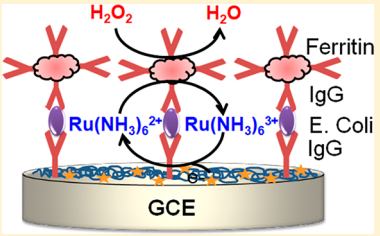

Ferritin is a 24-subunit protein that contains up to 4500 iron atoms in its hollow, in the form of a Fe(O)OH-type mineral core.[1] It possesses some unique features, such as safe iron reservoir,[2] rapid mineralization capability,[3] nanosynthesis capability within engineered protein cage,[4] mineralization possibility of variety of minerals within its cage,[5] and peroxidase mimicking activity.[6] Although ferritin itself is not a redox active protein, the redox status of the iron in the ferritin core can be altered,[7] and it shows some electrochemical signature since an electron transfer step is involved in the formation and dissolution of the iron core.[1] Thus, it has been used for determining intracellular localization of antigen through labeling with the antibody.[8] However, the bulk structural features and transient electrochemical properties of ferritin limit its broad utility in developing sensitive electrochemical bioassays. To improve the electrochemical redox behavior of ferritin, many approaches have been developed by modifying the electrode with self-assembled monolayers,[9,10] porous nanostructured film,[11] and electrodeposited nanoparticles,[12] or forming ferritin-contained composite with conducting materials such as carbon nanotubes,[13] and conducting polymer.[14] Although these strategies have significantly improved its redox properties, the practicability in electrochemical and photoelectrochemical bioassays is still challenging due to insufficient sensitivity.[15,16] Thus, the strategies to amplify the ferritin-triggered electrochemical signal is highly appealing.

Recently, a number of redox cycling schemes compatible with the electrochemical biosensing platform have been designed as signal amplification strategies to improve the performance of biosensors.[17] Among those strategies, outersphere-to-innersphere redox reaction as a signal enhancement concept exhibits both high signal amplification factor and low electrochemical background.[18] This concept can integrate the specificity of outersphere reaction-philic (OSR-philic) and innersphere reaction-philic (ISR-philic) redox couples, and suppress many theoretically possible reactions by maintaining the difference of OSR-philic/ISR-philic natures to obtain a high signal-to-background ratio, thus showing improved immunoassay performances in real applications.[19,20] By introducing a highly ISR-philic redox enzyme to trigger an electrochemical enzymatic redox scheme, an outersphere-to-innersphere redox reaction, the integrated electrochemical-chemical-enzymatic (ECN) redox cycling, has been achieved to significantly enhance enzymatic signal and lower the background.[21] However, these schemes suffer a problem using an OSR-philic redox couple with high formal potentials ($E^{0\prime}$) to reduce the highly OSR-philic signaling mediator with lower $E^{0\prime}$,[18−21] which complicates the theoretical feasibility of the outersphere-to-innersphere reaction mechanism. Thus, searching an OSR-philic redox couple with the $E^{0\prime}$ appropriate to OSR/ISR-philic redox couple is crucial in achieving full advantages of highly specific outersphere-to-innersphere redox reaction. Considering

Received: February 28, 2018
Accepted: June 4, 2018
Published: June 4, 2018

DOI: 10.1021/acs.analchem.8b00933
Anal. Chem. 2018, 90, 8028−8034

the fast oxidation of ferritin by the eco-friendly oxidant O_2 or H_2O_2[22] and the OSR/ISR-philic natures of ferritin, this work used ferritin as a label to develop an outersphere-to-innersphere redox reaction for highly sensitive immunoassay through matching an appropriate OSR-philic redox mediator to perform the primary electrochemical reaction on OSR-philic immunosensor surface.

The excellent peroxidase-mimicking activity of ferritin has been used for sandwich immunoassay with phenylenediamine[6] and hydroquinone[23] as substrate, respectively. However, these substrates are not the appropriate OSR-philic mediators, and the instability of phenolic or organic substrates with commonly generated radical oxygen species from the degradation of any H_2O_2 related system[24,25] also brings unpredictable background. To achieve ferritin-triggered outersphere-to-innersphere redox cycling, this work screened out a highly OSR-philic mediator $Ru(NH_3)_6^{3+}$ (Figure 1A) according to the needs of $E^{0\prime}$ lower

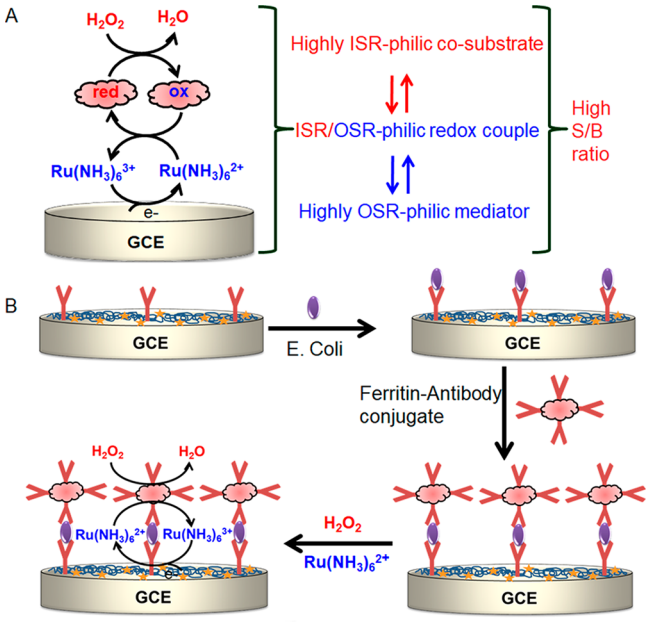

Figure 1. Schematic illustration of (A) OSR/ISR-controlled redox cycling mechanism, and (B) preparation of electrochemical immunosensor and immunoassay procedure with ferritin triggered redox cycling.

than that of ferritin, low reactivity with radical oxygen species, and quick electron exchange with ferritin redox couple. The fast innersphere reaction in ferritin-H_2O_2 system can keep ferritin in oxidized form to oxidize the highly OSR-philic mediator ($Ru(NH_3)_6^{2+}$), which opens a new avenue for highly sensitive electrochemical immunoassay (Figure 1B). Compared to the previous report,[21] the suggested scheme possessed theoretical feasibility and simplified the detection system. Using Enteropathogenic coli (*E. coli*) antigen, produced from the different strains of *E. coli* bacteria, a food borne pathogen,[26−28] as a model analyte, the designed outersphere-to-innersphere redox reaction showed high signal amplification efficiency, and the proposed immunoassay method showed high sensitivity and wide dynamic range, indicating the promising application of the ferritin-triggered redox cycling in amplified biosensing.

EXPERIMENTAL SECTION

Materials and Reagents. Glutaraldehyde (GA), $[Ru(NH_3)_6]Cl_3$, $[Ru(NH_3)_6]Cl_2$, and ferritin (from equine spleen, type-1) were purchased from Sigma-Aldrich Co. (U.S.A.). *E. coli* lipopolysaccharide protein antigen (purified by HPLC), mouse anti-*E. coli* antibody (AY-07718M) and rabbit anti-*E. coli* antibody (AY-07718R) were purchased from Shanghai Anyan Trading Co. Ltd. (Shanghai, China). Bovine serum albumin (BSA) was from KeyGEN Biotech. O. Ltd. (Nanjing, China). Chitosan was obtained from KAYON. Hydrogen peroxide (H_2O_2) was obtained from Shanghai Zhanyun Chemicals Co. Ltd. (Shanghai, china). 4-Amino-1-napthol hydrochloride was purchased from TCI (Shanghai, China). Methylene blue, acetic acid, nitric acid, acetone hydroxylamine·HCl, and ethylenediaminetetraacetic acid (EDTA) (CAS[6381-92-8]) were from Nanjing Chemical Reagent Co., Ltd. (Nanjing, China). Sulfosuccinimidyl-4-[*N*-maleimidomethyl] cyclohexane-1-carboxylate (sulfo-SMCC) and *N*-succinimidyl-S-acetylthiopropionate (SATP) were obtained from Thermo Scientific Inc. 50 K centrifuge filter was purchased from Merck Milipore Ltd. (Tullagreen, Ireland). Washing buffer contained PBS and 0.05% tween-20, and blocking buffer contained PBS and 5% BSA, which were obtained from Sigma-Aldrich Co. (U.S.A.).

Apparatus. Electrochemical measurements were carried out using CHI 660B (CH Instruments, Inc., Austin, TX, U.S.A.). All electrochemical experiments were carried out in a cell containing 10 mL 10 mM pH 7.4 PBS, a platinum wire as auxiliary, a Ag/AgCl (3 M NaCl) electrode as reference and a modified glassy carbon electrode (GCE, 3 mm in diameter) as working electrodes. Prior to modification, the GCE was polished to a mirror-like finish with 0.3 and 0.05 mm alumina slurry (Beuhler) followed by rinsing thoroughly with doubly distilled water, and then successively sonicated in 1:1 nitric acid, acetone, and doubly distilled water, and allowed to dry at room temperature.

Preparation of Immunosensor. The immunosensor was prepared following previous report[26] with some modification. In brief, 20 μL of 0.25 mg/mL chitosan in 0.1 M acetic acid was casted on a pretreated GCE and dried at room temperature for 1 h, which was then dipped in 0.25% GA solution for 2 h to activate the chitosan film. After the activated film was washed with distilled water repeatedly, the electrode was incubated with 20 μL of mouse anti-*E. coli* antibody (200 μg/mL) for 3 h at 4 °C. Afterward, the surface was washed with distilled water to remove unbound antibody for obtaining the immunosensor, which was shortly immersed in blocking buffer containing 5% BSA to block the active sites for minimizing the nonspecific binding.

Conjugation of Ferritin to Anti-*E. coli* Antibody. Ferritin-anti-*E. coli* antibody conjugate was prepared by cross-linking the $-NH_2$ groups of rabbit anti-*E. coli* antibody and ferritin. 500 μL of 200 μg/mL ferritin was first mixed with 50 μL of 1 mg/mL sulfo-SMCC in PBS to incubate for 30 min at room temperature, which was filtered by centrifugation at 10 000 rpm for 30 min through 50 K centrifuge filter, and the filtrate was dissolved in 500 μL PBS to obtain sulfo-SMCC-conjugated ferritin solution. Meanwhile, 500 μL of 200 μg/mL rabbit anti-*E. coli* antibody was mixed with 10 μL of 2 mg/mL SATP in PBS to incubate for 30 min at room temperature. The resulting solution was mixed with 20 μL of 0.012 g/mL EDTA and 0.044 g/mL hydroxyl-amine·HCl in PBS (pH 7.4) to incubate for 2 h at room temperature, which was then filtered

DOI: 10.1021/acs.analchem.8b00933
Anal. Chem. 2018, 90, 8028−8034

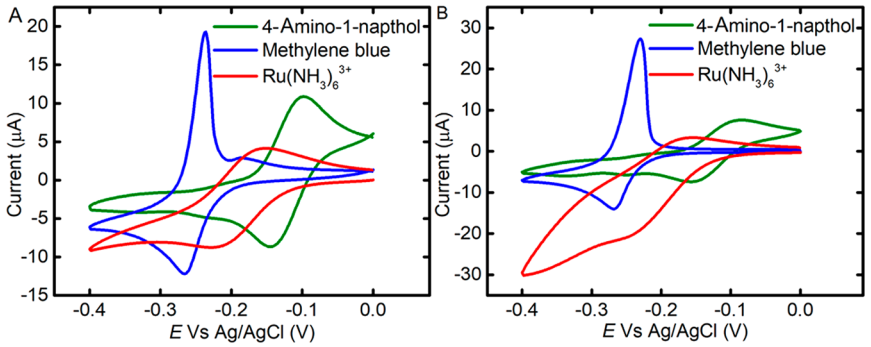

Figure 2. Cyclic voltammograms of 10 mM dissolved oxygen-free PBS (pH 7.4) containing marked species in (A) absence and (B) presence of 200 μg/mL ferritin and 10 mM H_2O_2 at bare GCE at 20 mV/s. The concentrations of $Ru(NH_3)_6^{3+}$, methylene blue, and 4-amino-1-napthol are 1.0 mM.

by centrifugation at 10 000 rpm for 30 min through 50 K centrifuge filter. The filtrate was dissolved in 500 μL of PBS to obtain the SATP-conjugated anti-*E. coli* antibody. After mixing the sulfo-SMCC-conjugated ferritin and the SATP-conjugated anti-*E. coli* antibody at a molar ratio of 1:1 for 2 h at room temperature, the mixture was centrifuged at 10 000 rpm for 30 min to obtain the ferritin-antibody conjugate, which was dissolved in 500 μL of blocking buffer.

Electrochemical Immunoassay. Twenty μL of sample or *E. coli* antigen at different concentrations was dropped on the immunosensor and left for 30 min at 4 °C for antigen−antibody binding. After washing with washing buffer, 20 μL of ferritin-antibody conjugate (200 μg/mL) was dropped on the surface and left for 30 min at 4 °C again. The surface was washed with washing buffer and then dipped in detection solution containing 10 mM PBS (pH 7.4), 1.0 mM $Ru(NH_3)_6^{2+}$, and 10.0 mM H_2O_2 for 30 min to perform the electrochemical measurement at room temperature (25 °C) without need of removing the dissolved oxygen.

RESULTS AND DISCUSSION

Screening of Highly OSR-philic Mediator for Ferritin-Triggered Redox Cycling. The ferritin-triggered redox cycling system was designed for signal amplification due to its OSR/ISR-philic natures (Figure 1A). The ISR-philic redox cycling could be performed by the fast oxidation of ferritin by the eco-friendly H_2O_2. To screen out a suitable mediator for performing the OSR-philic redox cycling on OSR-philic immunosensor surface, its $E^{0\prime}$ value, reactivity with radical oxygen species, and electron exchange rate with oxidized ferritin should be considered. According to the first condition, the $E^{0\prime}$ value of the mediator should be lower than that of ferritin. Thus, three commonly used mediators, $Ru(NH_3)_6^{3+}$, methylene blue and 4-amino-1-napthol, were first examined. As shown in Figure 2A, all of them showed a couple of redox peaks, from which the $E^{0\prime}$ values were calculated from the average of cathodic and anodic peak potentials to be −0.191, −0.251, and −0.121 V, respectively. Upon mixing with ferritin and H_2O_2, only $Ru(NH_3)_6^{3+}$ showed significant amplification of the reduction signal from −8.92 μA to −21.33 μA and slight decrease of the oxidation signal from 4.13 μA to 3.27 μA, while OSR-philic methylene blue[29] and 4-amino-1-napthol[20] showed slight change of both reduction and oxidation signals (Figure 2B). This could be attributed to the fast electron transfer of outersphere to innersphere redox reaction of highly OSR-philic species, $Ru(NH_3)_6^{3+}$, on OSR-philic GCE,[21] the instability of methylene blue[24] and phenolic mediator[25] influenced by unwanted generation of minute radical oxygen species, and the similar $E^{0\prime}$ of 4-amino-1-napthol to ferritin. So $Ru(NH_3)_6^{3+}$ could be considered as an appropriate mediator with its highly OSR-philic properties, $E^{0\prime}$ and high resistant against radical oxygen species of H_2O_2 related system, which ensured high signal amplification by redox cycling with minute background signal. To define the exact concentration of H_2O_2 and minimize its degradation, freshly prepared H_2O_2 solution was used.

Feasibility of Ferritin-Triggered Redox Cycling. The feasibility of electro-reduction-based ferritin-triggered redox cycling was first confirmed by examining the $E^{0\prime}$ values and OSR/ISR-philicity of these redox couples. From the cyclic voltammogram of ferritin, the $E^{0\prime}$ of ferritin redox couple was calculated to be −0.119 V vs Ag/AgCl (Figure S1 of the Supporting Information, SI). The $E^{0\prime}$ of H_2O_2/ H_2O is reported to be +1.77 V (vs SHE),[30,31] corresponding to +1.56 V vs Ag/AgCl. Considering $Ru(NH_3)_6^{3+}$ as the appropriate redox mediator with $E^{0\prime}$ lower than that of ferritin redox couple, the complete ferritin-triggered redox system at −0.23 V of GCE could be expressed in Figure 3A. The electrochemical signal

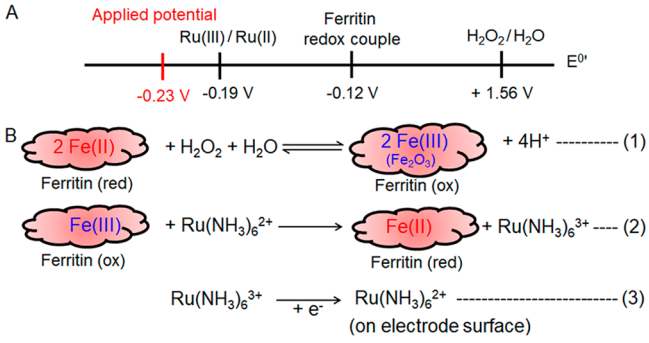

Figure 3. (A) Relative formal potentials (vs Ag/AgCl) of redox couples and (B) reactions involved in immunoassay.

was achieved through the specific reactions among the redox couples, by means of the outersphere-to-innersphere reaction mechanism and the suppression of OSR-philic/ISR-philic natures to theoretically possible reactions. The latter led to low background in conventional ferritin labeled sandwich immunoassay platform. The reaction specificity involved in the ferritin-triggered redox system was also confirmed by maintaining the OSR/ISR-philicity according to the following manner as OSR-philic GCE, highly OSR-philic $Ru(NH_3)_6^{3+}$/ $Ru(NH_3)_6^{2+}$ redox couple, OSR/ISR-philic ferritin redox couple and highly ISR-philic H_2O_2. The highly ISR-philic H_2O_2 was evaluated by its inner sphere reaction mechanism

DOI: 10.1021/acs.analchem.8b00933
Anal. Chem. 2018, 90, 8028−8034

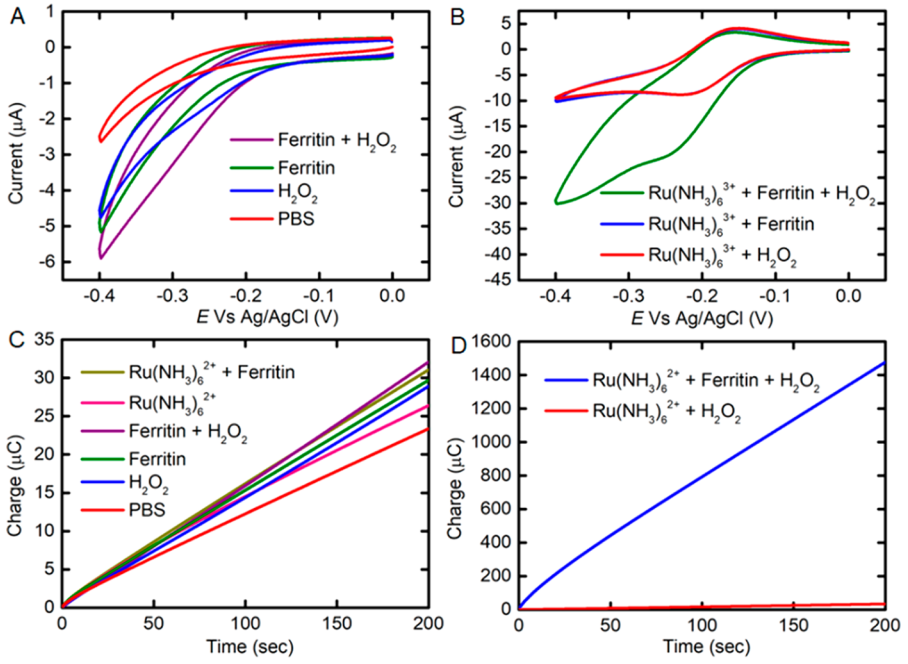

Figure 4. (A, B) Cyclic voltammograms of 10 mM PBS (pH 7.4) containing marked species at GCE at 20 mV/s and (C, D) chronocoulograms of 10 mM PBS (pH 7.4) containing marked species at GCE at −0.23 V. The concentrations of $Ru(NH_3)_6^{3+}$, $Ru(NH_3)_6^{2+}$, H_2O_2 and ferritin are 1.0 mM, 1.0 mM, 10 mM, and 200 μg/mL, respectively.

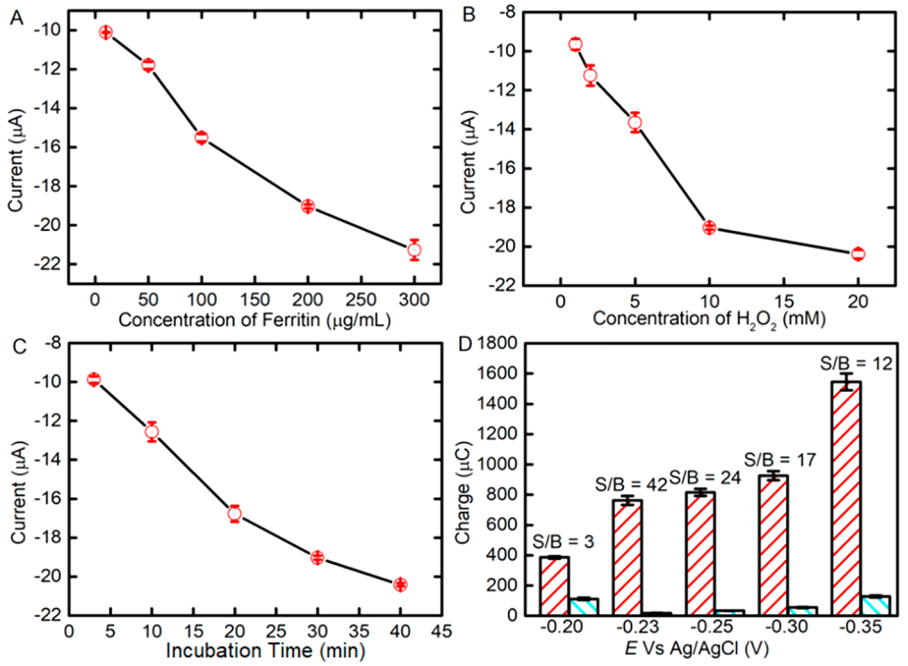

Figure 5. Plots of voltammetric response of (A) 1.0 mM $Ru(NH_3)_6^{2+}$ + 10.0 mM H_2O_2 vs ferritin concentration, (B) 1.0 mM $Ru(NH_3)_6^{2+}$ + 200.0 μg/mL ferritin vs H_2O_2 concentration and (C) 1.0 mM $Ru(NH_3)_6^{2+}$ + 10.0 mM H_2O_2 + 200 μg/mL ferritin vs incubation time, and (D) chronocoulometric response of 1.0 mM $Ru(NH_3)_6^{2+}$ + 10 mM H_2O_2 in presence and absence of 200 μg/mL ferritin as signal (cyan) and background (red) (n = 3), respectively, after applying different potentials for 100 s. The working electrode is bare GCE, and incubation time for A, B, and D is 30 min.

with ferritin[22] (Figure 3B), high reduction overpotential and slow electron transfer on OSR-philic GCE (Figure 4A, C). Although ferritin showed low response on OSR-philic GCE (Figure 4A, C), in support of highly ISR-philic H_2O_2, the fastly oxidized ferritin underwent fast chemical reduction by highly OSR-philic $Ru(NH_3)_6^{2+}$ (Figure 3B), indicating its OSR/ISR-philicity. So electrochemical reduction of chemically generated $Ru(NH_3)_6^{3+}$ (Figure 3B) via the redox cycling of $Ru(NH_3)_6^{2+}$ with ferritin and H_2O_2 produced high electrochemical readout on GCE (Figure 4B, D). Moreover, the low electrochemical response of ferritin at low scan rate (Figure 4A) and well-defined peak at high scan rate (Figure S1) indicated that no structural deformation occurred. For the sake of simplicity, the chronocoulometric reduction charge was plotted on positive Y-

DOI: 10.1021/acs.analchem.8b00933
Anal. Chem. 2018, 90, 8028−8034

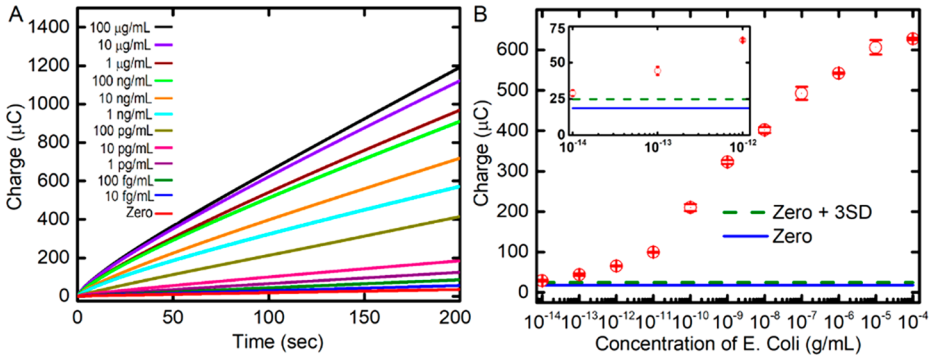

Figure 6. (A) Chronocoulograms of immunosensors in 10 mM PBS (pH 7.4) containing 1.0 mM $Ru(NH_3)_6^{2+}$ and 10.0 mM H_2O_2 at −0.23 V after incubation with *E. coli* at marked concentrations for 30 min and then ferritin-antibody for 30 min at 4 °C. (B) Plot of the response at 100 s vs logarithm of *E. coli* concentration. The inset represents a magnification of the plot at low concentrations of *E. coli*.

Table 1. Comparison of Detection Results with Other Redox Cycling-Based Immunoassay and Ferritin-Labeled Bioassays

detection method	target	biosensing strategy	detectable range	detection limit	ref
spectroscopy	human ceruloplasmin	ferritin-antibody	33 pM −3.3 nM	30 pM	6
chronocoulometry	CEA	tyrosinase-redox cycling	1 pg/mL to 50 μg/mL	1.0 fg/mL	21
voltammetry	CA 15−3	ferritin-CNTs -antibody	0.05−100 U/mL	0.009 U/mL	23
chronocoulometry	PfHRP2	methylene blue-redox cycling	10.0 fg/mL to 100 ng/mL	10.0 fg/mL	29
fluorescence	PDGF-BB	ferritin-glycine-rich peptide-eGFP	10 pM to 1.0 nM	100 fM	32
spectroscopy	cTnI	repebody-ferritin nanoparticles	1 pg/mL to 1 μg/mL	0.8 pg/mL	33
voltammetry	TNF-α	apoferritin tamplted metal phosphate NPs	10 pg/mL to 10 ng/mL	2 pg/mL	34
magnetic separation	erythrocyte	ferritin-concanavalin A	1−15 μg/mL		35
chronocoulometry	CA-125	GOx-redox cycling	0.1−100 U/mL	0.1 U/mL	36
chronocoulometry	PSA	GOx-redox cycling	10 pg/mL to 100 ng/mL	10 pg/mL	37
chronocoulometry	cTnI	GPDH-redox cycling	10 pg/mL to 100 ng/mL	10 pg/mL	38
chronocoulometry	CKMB	Au NP-redox cycling	100 fg/mL-10 ng/mL	20.0 fg/mL	39
chronocoulometry	PTH	nonenzymatic and diaphorase redox cycling	10 pg/mL to 100 ng/mL	2.0 pg/mL	40
chronocoulometry	PTH	nonenzymatic and Pd-NP redox cycling	1 pg/mL to 10 ng/mL	0.3 pg/mL	41
chronocoulometry	*E. coli* antigen	ferritin-redox cycling	10.0 fg/mL to 100 ng/mL	10.0 fg/mL	this work

scale. The similar electrochemical response of $Ru(NH_3)_6^{3+}$ and after mixing with ferritin (Figure 4B, C) also indicated that the ferroxidase activity of ferritin did not impact the reaction system. The complete schematic mechanism of ferritin-triggered redox system considering OSR/ISR-philicity of redox couples was presented in Figure 1B.

Optimization for High Electrochemical Signal-to-Background Ratio. To achieve the greatest signal amplification, the maximum electrochemical S/B ratio and the highest sensitivity of ferritin-triggered redox cycling for immunosensing application, the concentrations of the redox couples, incubation time, the applied potential were optimized. The immunosensing system required the addition of $Ru(NH_3)_6^{2+}$ and H_2O_2 to the detection solution, and ferritin was used as a label of biorecognition element to produce detection signal. Therefore, the response of $Ru(NH_3)_6^{2+}$ and H_2O_2 mixed in detection solution could be considered as the electrochemical background. With the increasing ferritin concentration, the CV response of 10 mM PBS (pH 7.4) containing 1 mM $Ru(NH_3)_6^{3+}$ and 10 mM H_2O_2 at −0.23 V quickly increased up to 100 μg/mL ferritin and then trended to a maximum increment value at 200 μg/mL (Figures S2A and 5A). Thus, 200 μg/mL ferritin was used as an optimum condition. The effect of H_2O_2 concentration on CV response of 10 mM PBS (pH 7.4) containing 1 mM $Ru(NH_3)_6^{3+}$ and 200 μg/mL ferritin showed similar tendency (Figure S2B), which gave the optimum H_2O_2 concentration at 10 mM (Figure 5B). Interestingly, the concentration variation of H_2O_2 did not affect the electrochemical background (Figure S3), thus H_2O_2 at the optimized concentration did not show any detrimental effect on ferritin. Due to the deeply imbedded iron core of ferritin within the structure, which lowered the electron transfer rate between ferritin redox couple and $Ru(NH_3)_6^{2+}$ or H_2O_2 in the detection solution, an incubation step was required to produce the high electrochemical readout. With the increasing incubation time, the CV response of 10 mM PBS (pH 7.4) containing 1 mM $Ru(NH_3)_6^{3+}$, 200 μg/mL ferritin and 10 mM H_2O_2 increased (Figure S2C) and trended to the maximum increment value at 30 min (Figure 5C), which was considered as optimum incubation time for the bioassay.

At the optimum concentrations of redox couples and incubation time, the applied potential for the ferritin-triggered redox cycling was optimized to be −0.23 V (Figure S4), at which the maximum electrochemical S/B ratio of 42 could be obtained (Figure 5D). Here the chronocoulometric readout at 100 s was used to calculate the electrochemical S/B ratio. Since chronocoulometry showed better reproducibility of the accumulated electrochemical signal and improved immunosensing performance than cyclic voltammetry for redox cycling based bioassay,[18] the following immunoassay was performed using chronocoulometry at −0.23 V.

***E. coli* Immunosensing with Ferritin-Triggered Redox Cycling.** To examine the application of the ferritin-triggered redox cycling in highly sensitive immunoassay, *E. coli* lipopolysaccharide protein antigen (purified by HPLC) was used as a model analyte, for which mouse anti-*E. coli* antibody

DOI: 10.1021/acs.analchem.8b00933
Anal. Chem. 2018, 90, 8028−8034

was immobilized on GCE surface as capture antibody, and rabbit anti-*E. coli* antibody was labeled with ferritin as detection probe of the traditional sandwich immunoassay. The performance of the detection probe was first evaluated (Figure S5). The charge response of ferritin in the mixture of $Ru(NH_3)_6^{3+}$ and H_2O_2 upon its conjugation to antibody showed minute change (from 793 μC to 759 μC), indicated insignificant impact of antibody on its catalytic activity and stability. The chronocoulometric response of the immunosensor showed continuous increment with the increasing *E. coli* concentration (Figure 6A). The plot of the response at 100 s vs the logarithm of *E. coli* concentration showed a good linearity in the range of 10.0 pg/mL to 0.1 μg/mL (Figure 6B). The detection limit was calculated at 3SD to be 10 fg/mL, according to the IUPAC definition: average of the detection signals from the negative control samples plus 3 times the standard deviation of the negative control signals. Although the detection limit of 10 fg/mL for *E. coli* antigen was 1 order of magnitude worse than that of 1 fg/mL for carcinoembryonic antigen (CEA) in previously reported tyrosinase-triggered redox scheme due to the difference of analytes,[21] the sensitivity of the proposed chronocoulometric immunoassay, the slope of signal enhancement at 10 pg/mL (1.1×10^{-4} C, Figure 6), was 1 order of magnitude higher than that of 1.2×10^{-5} C for the tyrosinase-triggered redox scheme, which was due to the theoretical feasibility of the proposed redox scheme and the faster redox reaction. The high sensitivity indicated the improved analytical performance of the ferritin-triggered redox cycling. It is anticipated that the developed ferritin-triggered redox cycling also offered high superiority over other ferritin labeled bioassays as well as improved biosensing performance over other redox cycling based immunoassays (Table 1). Although the proposed scheme exhibited similar sensitivity to the electro-oxidation based redox scheme[29] where methylene blue was used as label and TCEP as reductant, it offered advantages of theoretical feasibility and negligible interference of dissolved O_2 through its electro-reduction based assay. Moreover, it opens a new avenue for using ferritin as an efficient label for biosensing.

The practicability of the developed immunosensing method was demonstrated by testing commercial milk containing *E. coli* antigen. Five samples of commercial milk were prepared by spiking various concentration of *E. coli* antigen directly to the commercial milk to measure the chronocoulometric responses (Figure S6A). The matrices in the milk samples showed ignorable effect on the immunoassay of *E. coli* antigen (Figure S6B). The excellent reproducibility at different concentrations and wide detection range of the immunosensor indicated its superior practicability in sensitive detection of food borne pathogens from commercial sources.

CONCLUSIONS

This work reports a concept of ferritin-triggered redox cycling for significant electrochemical signal amplification. By using $Ru(NH_3)_6^{3+}$ as an OSR-philic redox mediator and H_2O_2 as an ISR-philic oxidant, the detection system shows excellent resistant of the mediator against radical oxygen species, and thus negligible background. The designed outersphere-to-innersphere redox reaction can produce greatly amplified electrochemical response, which leads to high S/B ratio for ferritin labeled immunosensing. Using *E. coli* antigen as a model analyte, the immunosensing method based on ferritin-triggered redox cycling shows excellent performance with greatly improved sensitivity. This work opens a new avenue to use ferritin as an efficient label of traditional biosensor for developing highly sensitive methodology for bioanalysis.

ASSOCIATED CONTENT

Supporting Information

The Supporting Information is available free of charge on the ACS Publications website at DOI: 10.1021/acs.analchem.8b00933.

Cyclic voltammogram of ferritin at GCE, optimization of redox cycling parameters, evaluation of H_2O_2 impact, activity evaluation of ferritin-antibody conjugate, and detection of *E. coli* in commercial milk (PDF)

AUTHOR INFORMATION

Corresponding Author

*Phone/Fax: +86-25-89683593. E-mail: hxju@nju.edu.cn (H.X.J.).

ORCID

Md. Rajibul Akanda: 0000-0002-9529-0578

Huangxian Ju: 0000-0002-6741-5302

Present Address

[†]Permanent address: Department of Chemistry, Jagannath University, Dhaka-1100, Bangladesh

Notes

The authors declare no competing financial interest.

ACKNOWLEDGMENTS

This work was financially supported by the National Natural Science Foundation of China (21635005, 21361162002).

REFERENCES

(1) Jutz, G.; van Rijn, P.; Santos Miranda, B.; Böker, A. *Chem. Rev.* **2015**, *115*, 1653−1701.

(2) Marchetti, A.; Parker, M. S.; Moccia, L. P.; Lin, E. O.; Arrieta, A. L.; Ribalet, F.; Murphy, M. E. P.; Maldonado, M. T.; Armbrust, E. V. *Nature* **2009**, *457*, 467−470.

(3) Tosha, T.; Hasan, M. R.; Theil, E. C. *Proc. Natl. Acad. Sci. U. S. A.* **2008**, *105*, 18182−18187.

(4) Kramer, R. M.; Li, C.; Carter, D. C.; Stone, M. O.; Naik, R. R. *J. Am. Chem. Soc.* **2004**, *126*, 13282−13286.

(5) Yamashita, I.; Iwahori, K.; Kumagai, S. *Biochim. Biophys. Acta, Gen. Subj.* **2010**, *1800*, 846−857.

(6) Tang, Z.; Wu, H.; Zhang, Y.; Li, Z.; Lin, Y. *Anal. Chem.* **2011**, *83*, 8611−8616.

(7) Watt, G. D.; Jacobs, D.; Frankel, R. B. *Proc. Natl. Acad. Sci. U. S. A.* **1988**, *85*, 7457−7461.

(8) Olsen, B. R.; Berg, R. A.; Kishida, Y.; Prockop, D. J. *Science* **1973**, *182*, 825−827.

(9) Wu, Y.; Hu, S. *Anal. Chim. Acta* **2004**, *527*, 37−43.

(10) Ritzert, N. L.; Casella, S. S.; Zapien, D. C. *Electrochem. Commun.* **2009**, *11*, 827−830.

(11) Yang, X.; Yuan, R.; Chai, Y.; Zhuo, Y.; Hong, C.; Liu, Z.; Su, H. *Talanta* **2009**, *78*, 596−601.

(12) Moghaddam, A. B.; Esmaieli, M.; Khodadadi, A. A.; Ganjkhanlou, Y.; Asheghali, D. *Microchim. Acta* **2011**, *173*, 317−322.

(13) Shin, K. M.; Lee, J. W.; Wallace, G. G.; Kim, S. J. *Sens. Actuators, B* **2008**, *133*, 393−397.

(14) Inamuddin; Shin, K. M.; Kim, S. I.; So, I.; Kim, S. J. *Electrochim. Acta* **2009**, *54*, 3979−3983.

(15) Qiu, Z.; Shu, J.; Tang, D. *Anal. Chem.* **2018**, *90*, 1021−1028.

(16) Shu, J.; Tang, D. *Chem. - Asian J.* **2017**, *12*, 2780−2789.

(17) Yang, H. *Curr. Opin. Chem. Biol.* **2012**, *16*, 422−428.

(18) Akanda, M. R.; Choe, Y.-L.; Yang, H. *Anal. Chem.* **2012**, *84*, 1049−1055.

DOI: 10.1021/acs.analchem.8b00933
Anal. Chem. 2018, 90, 8028−8034

(19) Akanda, M. R.; Tamilavan, V.; Park, S.; Jo, K.; Hyun, M. H.; Kim, S.; Yang, H. *Anal. Chem.* **2013**, *85*, 1631−1636.
(20) Akanda, M. R.; Joung, H.-A.; Tamilavan, V.; Park, S.; Kim, S.; Hyun, M. H.; Kim, M.-G.; Yang, H. *Analyst* **2014**, *139*, 1420−1425.
(21) Akanda, M. R.; Ju, H. X. *Anal. Chem.* **2017**, *89*, 13480−13486.
(22) Liu, X.; Theil, E. C. *Acc. Chem. Res.* **2005**, *38*, 167−175.
(23) Akter, R.; Jeong, B.; Choi, J.-S.; Rahman, M. A. *Biosens. Bioelectron.* **2016**, *80*, 123−130.
(24) Sánchez, L. D.; Taxt-Lamolle, S. F. M.; Hole, E. O.; Krivokapić, A.; Sagstuen, E.; Haugen, H. J. *Appl. Catal., B* **2013**, *142*−*143*, 662−667.
(25) Soltani, T.; Entezari, M. H. *Chem. Eng. J.* **2014**, *251*, 207−216.
(26) Buchana, R. L.; Doyle, M. P. *Food Technol.* **1997**, *51*, 69−75.
(27) Ochoa, T. J.; Contreras, C. A. *Curr. Opin. Infect. Dis.* **2011**, *24*, 478−483.
(28) Akanda, M. R.; Ju, H. X. *Anal. Chem.* **2016**, *88*, 9856−9861.
(29) Dutta, G.; Lillehoj, P. B. *Analyst* **2017**, *142*, 3492−3499.
(30) Jing, X.; Cao, D.; Liu, Y.; Wang, G.; Yin, J.; Wen, Q.; Gao, Y. *J. Electroanal. Chem.* **2011**, *658*, 46−51.
(31) Blattner, F. R.; Plunkett, G.; Bloch, C. A.; Perna, N. T.; Burland, V.; Riley, M.; Collado-Vides, J.; Glasner, J. D.; Rode, C. K.; Mayhew, G. F.; Gregor, J.; Davis, N. W.; Kirkpatrick, H. A.; Goeden, M. A.; Rose, D. J.; Mau, B.; Shao, Y. *Science* **1997**, *277*, 1453−1462.
(32) Kim, S.-E.; Ahn, K.-Y.; Park, J.-S.; Kim, K. R.; Lee, K. E.; Han, S.-S.; Lee, J. *Anal. Chem.* **2011**, *83*, 5834−5843.
(33) Men, D.; Zhang, T.-T.; Hou, L.-W.; Zhou, J.; Zhang, Z.-P.; Shi, Y.-Y.; Zhang, J.-L.; Cui, Z.-Q.; Deng, J.-Y.; Wang, D.-B.; Zhang, X.-E. *ACS Nano* **2015**, *9*, 10852−10860.
(34) Liu, G.; Wu, H.; Wang, J.; Lin, Y. *Small* **2006**, *2*, 1139−1143.
(35) Owen, C. S.; Lindsay, J. G. *Biophys. J.* **1983**, *42*, 145−150.
(36) Singh, A.; Park, S.; Yang, H. *Anal. Chem.* **2013**, *85*, 4863−4868.
(37) Dutta, G.; Kim, S.; Park, S.; Yang, H. *Anal. Chem.* **2014**, *86*, 4589−4595.
(38) Dutta, G.; Park, S.; Singh, A.; Seo, J.; Kim, S.; Yang, H. *Anal. Chem.* **2015**, *87*, 3574−3578.
(39) Fang, C. S.; Oh, K. W.; Oh, A.; Lee, K.; Park, S.; Kim, S.; Park, J. K.; Yang, H. *Chem. Commun.* **2016**, *52*, 5884−5887.
(40) Kang, C.; Kang, J.; Lee, N.-S.; Yoon, Y. H.; Yang, H. *Anal. Chem.* **2017**, *89*, 7974−7980.
(41) Nandhakumar, P.; Kim, B.; Lee, N.-S.; Yoon, Y. H.; Lee, K.; Yang, H. *Anal. Chem.* **2018**, *90*, 807−813.

DOI: 10.1021/acs.analchem.8b00933
Anal. Chem. 2018, 90, 8028−8034